


ORIGINAL ARTICLE

Induction of potent antitumor immunity by intradermal DNA injection using a novel needle-free pyro-drive jet injector

Shinya Inoue¹ | Izuru Mizoguchi¹ | Jukito Sonoda¹ | Eri Sakamoto¹ |
Yasuhiro Katahira¹ | Hideaki Hasegawa¹ | Aruma Watanabe¹ |
Yuma Furusaka¹ | Mingli Xu¹ | Toshihiko Yoneto¹ | Naoki Sakaguchi² |
Kazuhiro Terai² | Kunihiko Yamashita² | Takayuki Yoshimoto¹ 

¹Department of Immunoregulation, Institute of Medical Science, Tokyo Medical University, Tokyo, Japan

²Department of Device Application for Molecular Therapeutics, Graduate School of Medicine, Osaka University, Osaka, Japan

Correspondence

Takayuki Yoshimoto, Department of Immunoregulation, Institute of Medical Science, Tokyo Medical University, 6-1-1 Shinjuku, Shinjuku-ku, Tokyo 160-8402, Japan.

Email: yoshimot@tokyo-med.ac.jp

Funding information

Daicel Corporation; Ministry of Education, Culture, Sports, Science and Technology, Japan

Abstract

The current success of mRNA vaccines against COVID-19 has highlighted the effectiveness of mRNA and DNA vaccinations. Recently, we demonstrated that a novel needle-free pyro-drive jet injector (PJI) effectively delivers plasmid DNA into the skin, resulting in protein expression higher than that achieved with a needle syringe. Here, we used ovalbumin (OVA) as a model antigen to investigate the potential of the PJI for vaccination against cancers. Intradermal injection of OVA-expression plasmid DNA into mice using the PJI, but not a needle syringe, rapidly and greatly augmented OVA-specific CD8⁺ T-cell expansion in lymph node cells. Increased mRNA expression of both interferon- γ and interleukin-4 and an enhanced proliferative response of OVA-specific CD8⁺ T cells, with fewer CD4⁺ T cells, were also observed. OVA-specific *in vivo* killing of the target cells and OVA-specific antibody production of both the IgG2a and IgG1 antibody subclasses were greatly augmented. Intradermal injection of OVA-expression plasmid DNA using the PJI showed stronger prophylactic and therapeutic effects against the progression of transplantable OVA-expressing E.G7-OVA tumor cells. Even compared with the most frequently used adjuvants, complete Freund's adjuvant and aluminum hydroxide with OVA protein, intradermal injection of OVA-expression plasmid DNA using the PJI showed a stronger CTL-dependent prophylactic effect. These results suggest that the novel needle-free PJI is a promising tool for DNA vaccination, inducing both a prophylactic and a therapeutic effect against cancers, because of prompt and strong generation of OVA-specific CTLs and subsequently enhanced production of both the IgG2a and IgG1 antibody subclasses.

KEYWORDS

antitumor immunity, DNA vaccine, generation of CTLs, intradermal injection, pyro-drive jet injector

Abbreviations: CFA, complete Freund's adjuvant; CFSE, carboxyfluorescein diacetate succinimidyl ester; DC, dendritic cell; IFN- γ , interferon gamma; OVA, ovalbumin; PJI, pyro-drive jet injector.

This is an open access article under the terms of the [Creative Commons Attribution-NonCommercial](https://creativecommons.org/licenses/by-nc/4.0/) License, which permits use, distribution and reproduction in any medium, provided the original work is properly cited and is not used for commercial purposes.

© 2022 The Authors. *Cancer Science* published by John Wiley & Sons Australia, Ltd on behalf of Japanese Cancer Association.

1 | INTRODUCTION

The current success of vaccination against COVID-19 has highlighted the therapeutic effectiveness of mRNA vaccines.¹ Compared with traditional protein-based and attenuated pathogen vaccines, which take time or sometimes are even difficult to produce, the nucleic acid–base mRNA and DNA vaccines have been considered to have several advantages: they can be rapidly developed, flexibly adapted to various mutations, and quickly produced on an industrial scale.² Moreover, the large-scale vaccination programs using the mRNA vaccines against COVID-19 have proved their efficacy and safety worldwide. Unlike DNA vaccines, mRNA vaccines are more unstable and degrade easily; a deep-freeze storage and logistics system is therefore needed for their distribution, which can be an obstacle to worldwide delivery.

The COVID-19 mRNA vaccines use intramuscular administration because it is easy to perform and generally well tolerated, with a low risk for adverse reactions at the injection site. In addition, muscle tissue has a generous blood supply, and therefore vaccine antigens administered into muscle are rapidly absorbed into the circulation. However, vaccine delivery to the skin has long been considered a superior strategy for amplifying the vaccine response because the skin has many resident DCs (including Langerhans cells and dermal DCs), lymph vessels, and blood capillaries.^{2,3} DCs, a specialized cell type with the most potent antigen-presenting ability in the immune system, play a major role in inducing and orchestrating the immune response. Indeed, accumulating evidence suggests that intradermal injection has several advantages that make it superior to intramuscular injection. For example, compared with intramuscular injection, intradermal injection of the yellow fever virus or influenza vaccines was observed to enhance the prophylactic immune response in healthy individuals and even in those whose response is otherwise nonexistent or low.⁴ Notably, intradermal vaccination has also been shown to allow for a reduced antigen dose without loss of efficacy.^{5,6} Moreover, intradermal administration of an mRNA vaccine more efficiently activates DCs at the site of injection, followed by a higher vaccine-specific T-cell response and greater antibody production.⁷

In contrast with the typical needle injection, needle-free injection offers several advantages that are useful in situations of large-scale vaccination or limited vaccine supply: dose-sparing because of intradermal efficiency, elimination of needle-stick injuries and cross-contamination by re-use, and lower healthcare costs.⁸ Very recently, we developed a novel needle-free PJI that has the advantage of adjustability in the dose delivered and depth of delivery through a choice between two types of explosive.^{9–12} Luciferase- and OVA-expression DNA were efficiently delivered to dermal tissue by intradermal injection with the PJI, and protein expression was found to be far higher than with a typical needle syringe.^{9,10} In addition, OVA-specific antibody production was greatly enhanced.¹⁰ Similarly, when the SARS-CoV-2 spike protein expression DNA was intradermally injected using the PJI, enhanced production of neutralizing antibodies to the virus and inhibition of viral infection in a mouse model were observed (Nishikawa et al., submitted).

In the present study, we investigated whether intradermal injection using the PJI can induce potent antitumor immunity in a mouse transplantable tumor model expressing OVA as a model antigen. Compared with injection using a needle syringe, intradermal injection of OVA-expression plasmid DNA using the PJI was observed to induce a much stronger antitumor immune response, with generation of antigen-specific CTLs, followed by killing of the target cells and antigen-specific antibody production. Those results indicate that the PJI is a promising tool for inducing antitumor immunity by DNA vaccination against cancers.

2 | MATERIALS AND METHODS

2.1 | Mice

C57BL/6 mice were purchased from Sankyo Labo Service. OT-I and OT-II T-cell receptor transgenic mice were kindly provided by, respectively, Dr. K. Takahashi (Yokohama City University) and Dr. T. Yoshimoto (Hyogo Medical University). All mice were maintained under pathogen-free conditions, and all animal experiments were approved by the President and the Institutional Animal Care and Use Committee of Tokyo Medical University and were performed in accordance with institutional, scientific community, and national guidelines for animal experimentation and the Animal Research: Reporting of In Vivo Experiments guidelines.

2.2 | Cell culture

E.G7 cells (CRL-2113), a derivative of EL-4 thymoma cells transfected with OVA cDNA, were purchased from the American Type Culture Collection (ATCC). E.G7 cells, lymph node cells, and spleen cells were cultured at 37°C under 5% CO₂/95% air in RPMI 1640 medium containing 10% FBS, L-glutamine (2 mM), penicillin (100 U/ml), streptomycin (100 µg/ml), and β-mercaptoethanol (50 µM).

2.3 | Intradermal injection using the PJI

The PJI (called Actranza) was provided by the Daicel Corporation, and 25 mg ignition powder and 40 mg smokeless powder were used for mice (Figure S1).^{9–12} After the mouse abdominal skin was shaved, 20 µl OVA-expression plasmid DNA (pOVA, 2 mg/ml; Addgene) or GFP-expression plasmid DNA (pGFP, GFP cDNA subcloned in the pCAGGS vector,¹³ provided from Dr. Miyazaki, 2 mg/ml) was intradermally injected into both the right and left flank areas (two sites each, total four sites/mouse) using the PJI or a needle syringe (Micro-Fine Insulin Syringe 30G × 8 mm needle; BD Biosciences). OVA protein in PBS (1 or 10 mg/ml; Sigma-Aldrich) was emulsified in an equal volume of CFA (BD Difco), and 100 µl of the emulsified mixture (CFA/OVA, 500 µg as a positive control or 50 µg for comparison with AlumVax) was subcutaneously injected

into two sites in both flanks. OVA protein (Sigma-Aldrich) in PBS (1 mg/ml) was mixed with an equal volume of 2% aluminum hydroxide (AlumVax Hydroxide: OZ Biosciences), and 100 μ l of OVA protein precipitated with AlumVax (alum/OVA, 50 μ g) according to the manufacturer's instruction was subcutaneously injected into two sites in both flanks.

2.4 | Cell transfer

Naive CD62L⁺CD8⁺ T cells were purified from spleen cells of OT-I mice using the naive CD8⁺ T Cell Isolation Kit and autoMACS Pro (Miltenyi Biotec). Naive CD62L⁺CD4⁺ T cells were purified from spleen cells of OT-II mice using the naive CD4⁺ T Cell Isolation Kit and autoMACS Pro (Miltenyi Biotec). The purity of the CD62L⁺CD8⁺ and CD62L⁺CD4⁺ T cells was routinely assessed at >95%. At 1 day before immunization, a mixture of both cells (1×10^5) in 200 μ l PBS was injected intravenously.

2.5 | Tetramer staining assay

Phycoerythrin (PE)-conjugated tetramers of MHC class I H-2K^b and its restricted peptide epitope of OVA (OVA₂₅₇₋₂₆₄ peptide, SIINFEKL) and of MHC class II I-A^b and its restricted peptide epitope of OVA (OVA₃₂₃₋₃₃₉ peptide, ISQAVHAAHAEINEAGR) were purchased from MBL. After immunization, draining inguinal lymph node cells were stained with the MHC class I-OVA peptide tetramer and FITC-conjugated anti-CD8 (KT15; MBL) or MHC class II-OVA peptide tetramer and FITC-conjugated anti-CD4 (GK1.5; BioLegend) according to the manufacturer's protocol. The resulting cells were analyzed using a FACSCanto II flow cytometer (BD Biosciences) and the FlowJo software application (version 10: Flo Jo). Flow cytometry gating strategy for the tetramer staining assay is shown in Figure S2A,B.

2.6 | FACS analysis of skin and lymph node cells

For detection of DCs presenting OVA peptide SIINFEKL in the MHC class I H-2K^b or GFP expression in the skin cells and lymph node cells, mice were intradermally injected with 20 μ l pOVA or pGFP (2 mg/ml, four sites each) using PJI or a needle syringe. At 24 or 48 h later, the mouse abdominal skin tissue was cut out and washed in PBS, minced, and treated with 1 mg/ml dispase II (FUJIFILM Wako Pure Chemical) in RPMI 1640 medium containing 5% FBS at 4°C overnight. The skin sample was further treated with 1 mg/ml collagenase (FUJIFILM Wako Pure Chemical) at 37°C for 2–3 h with shaking. After passing through a 70-mm strainer, the single-cell suspension of skin cells and lymph node cells was then stained with PE antimouse MHC class I H-2K^b bound to OVA peptide SIINFEKL antibody (25-D1.16),¹⁴ APC-Cy7-conjugated anti-CD11c (N418, BioLegend), and FITC- or APC-conjugated anti-MHC class

II (M5/114.15.2, BioLegend). For intracellular cytokine staining of lymph node cells, the single-cell suspension was restimulated for 4 h with 50 ng/ml PMA and 500 ng/ml ionomycin in the presence of 5 μ g/ml brefeldin A. Cells were stained with Pacific Blue-conjugated anti-CD4 (GK1.5, BioLegend) and APC-Cy7-conjugated anti-CD8 (53.6.8, BioLegend) for 15 min, then fixed with Fixation Buffer (eBioscience) overnight. Then, these cells were permeabilized with Permeabilization Buffer (eBioscience) and stained intracellularly with FITC-conjugated anti-IFN- γ (XMG1.2, BioLegend) and PE-conjugated anti-IL-4 (11B11, eBioscience) for 30 min. Resultant cells were analyzed on a FACSCanto II flow cytometer (BD Biosciences) followed by FlowJo software application.

2.7 | Real-time RT-PCR

Total RNA was prepared from draining inguinal lymph node cells using the RNeasy Mini Kit (Qiagen), and cDNA was prepared using the oligo(dT) primer and SuperScript IV Reverse Transcriptase (Invitrogen). Real-time quantitative PCR was performed using SYBR Premix Ex Taq II and a Thermal Cycler Dice real-time system (Takara) according to the manufacturer's instructions. Hypoxanthine guanine phosphoribosyl transferase (*HPRT*) was used as a housekeeping gene to normalize mRNA. Relative expression of real-time PCR products was determined using the $\Delta\Delta C_t$ method to compare mRNA expression of the target and housekeeping genes. The specific primer pairs used for each gene in the quantitative RT-PCR analysis were *IFN- γ* , 5'-CGGCACAGTCATTGAAAGCCTA-3' and 5'-GTTGCTGATGGCCTGATTGTC-3'; *interleukin 4 (IL-4)*, 5'-CCTGCTTACCAGAGATCTGTCC-3' and 5'-GAAGCCCTACAGACGAGCTCAC-3'; *HPRT*, 5'-TTGTTGTTGGATATGCCCTTGACTA-3' and 5'-AGGCAGATGGCCACAGGACTA-3' (TaKaRa).

2.8 | Western blot analysis

After intradermal injection of 20 μ l pOVA (5 mg/ml four sites each) using PJI, the mouse abdominal skin tissue was cut out, minced, and lysed in a RIPA buffer (20 mM Tris HCl pH 7.4, 150 mM NaCl, 1% Triton X-100, 1% sodium deoxycholate, and 0.1% SDS) containing protease inhibitor cocktail (Sigma-Aldrich) with sonicating. After centrifugation, protein concentration in the supernatant was determined using bicinchoninic acid (BCA) Protein Assay Kit (TaKaRa). The supernatant (5 μ g/lane) was separated on an SDS-PAGE under reducing conditions and transferred to a polyvinylidene difluoride membrane (Millipore, Bedford, MA). The membrane was then blocked, probed with anti-OVA (3G2E1D9, Santa Cruz) or anti-actin (Sigma-Aldrich), followed by antimouse IgG conjugated to horseradish peroxidase, and visualized with the enhanced chemiluminescence (ECL) detection system (Amersham Pharmacia Biotech) according to the manufacturer's instructions. Image capture was performed using the iBright FL1500 Imaging System (Thermo Fisher Scientific). The intensity of each band was quantified using ImageJ software (National Institutes of Health).¹⁵

2.9 | Proliferation assay

Draining inguinal lymph node cells (1×10^4 cells in $200 \mu\text{l}$) were stimulated in the presence or absence of $3 \mu\text{M}$ MHC class I H-2K^b-restricted OVA₂₅₇₋₂₆₄ peptide (Life Technologies) or MHC class II I-A^b-restricted OVA₃₂₃₋₃₃₉ peptide (Invitrogen) for 72 h. Cell proliferative activity was determined using the CellTiter-Glo 2.0 Cell Viability Assay (Promega), and luminescence intensity was measured using the GloMax Discovery Microplate Reader (Promega) according to the manufacturer's instructions.

2.10 | Serum antibody titer

Blood was collected by cardiac puncture and the resultant serum was analyzed for concentrations of OVA-specific total IgG and IgG1 and IgG2a subclasses by mouse anti-OVA antibody subtype/subclass ELISA kits (Chondrex; Bethyl Laboratories; Abcam). OVA protein was coated onto an ELISA plate at $10 \mu\text{g/ml}$ in a carbonate buffer and incubated at 4°C overnight. After the plate was blocked with 5% BSA, serially diluted serum samples were added onto the plate and incubated at 4°C overnight, and then further incubated with horseradish peroxidase-conjugated antimouse total IgG, IgG1, and IgG2a. Color development used a 3,3',5,5'-tetramethylbenzidine substrate set (BioLegend), and absorbance at 450 nm was detected in a microplate reader (iMark Microplate Reader: Bio-Rad).

2.11 | In vivo killing assay

C57BL/6 mouse splenocytes were incubated with and without MHC class I H-2K^b-restricted OVA₂₅₇₋₂₆₄ peptide (SIINFEKL, $1 \mu\text{M}$) at 37°C for 1 h and were washed with complete medium and PBS. The pulsed target splenocytes and unpulsed splenocytes were then incubated with, respectively, 5 and $0.5 \mu\text{M}$ CFSE (Invitrogen) at 37°C for 10 min with gentle agitation.¹⁶ After the cells were washed, an equal number of peptide-pulsed CFSE^{high} cells and unpulsed CFSE^{low} cells (2×10^6 cells each) were injected intravenously into mice vaccinated using the PJI or a needle syringe. At 4 h later, spleens were harvested and analyzed using a FACSCanto II flow cytometer and the FlowJo software application (version 10). The flow cytometry gating strategy for the in vivo killing assay is shown in Figure S2C.

2.12 | In vivo tumor growth

E.G7-OVA cells were harvested at the exponential growth phase and washed with PBS. Subsequently, 2×10^6 cells/ $100 \mu\text{l}$ were subcutaneously injected into right flank of C57BL/6 mice. Tumor size was measured daily using electronic calipers and was expressed as a volume (mm^3) using the volume equation $0.5(ab^2)$, in which a is the long diameter and b is the short diameter. For depletion of CD4⁺ T cells or

CD8⁺ T cells, each mouse was injected i.p. with 0.5 mg rat antimouse CD8 (53-6.7), anti-CD4 (GK1.5; all from the ATTC), or normal rat IgG (Sigma-Aldrich) as control antibody in $200 \mu\text{l}$ PBS 1 day before tumor inoculation, once daily for the following 5 consecutive days as reported.¹⁷

2.13 | Statistical analysis

Data are expressed as the mean \pm SEM for each group. Statistical analyses were performed in the GraphPad Prism software application (version 9; GraphPad Software), using the unpaired two-tailed Student *t*-test for comparisons involving two groups or a one- or two-way ANOVA with the Tukey multiple comparison test for comparisons involving three or more groups. A *p*-value < 0.05 was considered to indicate a statistically significant difference.

3 | RESULTS

3.1 | Intradermal injection of OVA-expression plasmid DNA with the PJI, but not a needle syringe, efficiently augmented OVA-specific CD8⁺ T cells

To investigate whether intradermal vaccination using the PJI can induce potent antitumor immunity, OVA was used as the model antigen. First, to increase sensitivity to OVA-specific immune responses, mice received intravenous injections of OT-I-derived naive CD8⁺ T cells and OT-II-derived naive CD4⁺ T cells 1 day before immunization (Figure 1A). The next day, the mice were intradermally injected once with OVA-expression plasmid DNA using the PJI or a needle syringe, together with PBS and the emulsified CFA/OVA protein as negative and positive controls, respectively. At 1 week later, draining lymph node cells were stained with MHC class I-OVA peptide tetramer and anti-CD8, or MHC class II-OVA peptide tetramer and anti-CD4. Injection using the PJI, but not a needle syringe, greatly augmented the frequency of OVA-specific CD8⁺ T cells (Figure 1B,D). However, the frequency of OVA-specific CD4⁺ T cells was just slightly enhanced after both types of injection (Figure 1C,E). As a positive control, injection of emulsified CFA/OVA protein efficiently augmented the frequencies of both T-cell types (Figure 1B-E). Consistent with those results, injection using the PJI, but not a needle syringe, greatly enhanced the mRNA expression of both IFN- γ and IL-4 in the draining lymph node cells (Figure 1F,G).

Next, to examine the recall antigen-specific response, the lymph node cells were restimulated with the MHC class I-restricted OVA₂₅₇₋₂₆₄ peptide or MHC class II-restricted OVA₃₂₃₋₃₃₉ peptide, and their proliferative response was determined. Injection using the PJI, but not a needle syringe, greatly induced antigen-specific proliferation in response to the MHC class I-OVA peptide, although injection with emulsified CFA/OVA protein failed to induce proliferation¹⁸⁻²⁰ (Figure 1H). In contrast, injection using the PJI only slightly

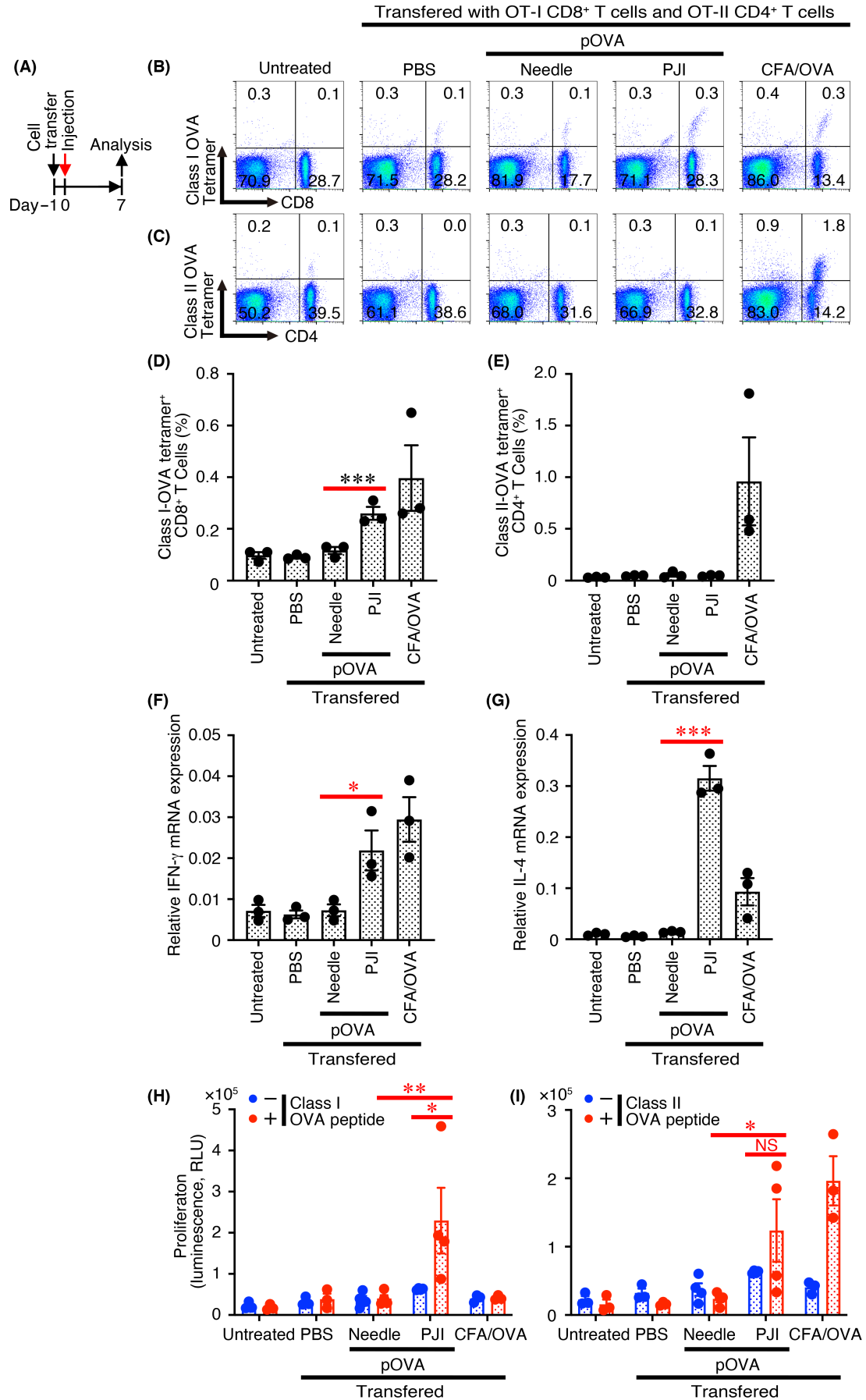


FIGURE 1 Intradermal injection of ovalbumin (OVA)-expression plasmid DNA with the pyro-drive jet injector (PJI), but not a needle syringe, efficiently augmented OVA-specific CD8⁺ T cells. (A) Mice intravenously injected with OT-I-derived naive CD8⁺ T cells and OT-II-derived naive CD4⁺ T cells 1 day before were then intradermally injected once with OVA-expression plasmid DNA (pOVA) using the PJI or a needle syringe, PBS, and OVA protein combined with complete Freund's adjuvant (CFA/OVA, 500 μg) as a positive control. At 1 week later, the draining lymph node cells were stained with OVA-specific MHC class I tetramer and anti-CD8, or OVA-specific MHC class II tetramer and anti-CD4. (B, C) Representative plots are shown, and (D, E) average percentages of positive cells were calculated and compared. mRNA expression of (F) IFN-γ and (G) IL-4 in the draining lymph nodes were compared. The draining lymph node cells were also stimulated in the presence or absence of (H) MHC class I-restricted OVA₂₅₇₋₂₆₄ peptide or (I) MHC class II-restricted OVA₃₂₃₋₃₃₉ peptide, and 72 h later, the proliferative response was determined. Data shown are the mean ± SEM (*n* = 3, D–G; *n* = 4, H, I) of three independent experiments. *p*-values were determined using one-way ANOVA with the Tukey test for multiple comparisons. **p* < 0.05, ***p* < 0.01, ****p* < 0.001.

induced proliferation in response to the MHC class II–OVA peptide, while injection of emulsified CFA/OVA protein greatly increased proliferation, probably because of its preferable activation of CD4⁺ T cells rather than CD8⁺ T cells^{18–20} (Figure 1). These results suggest that just a single intradermal injection of OVA-expression plasmid DNA using the PJI, but not a needle syringe, in transferred mice efficiently augmented the OVA-specific CD8⁺ T-cell response, and slightly augmented the specific CD4⁺ T-cell response in draining lymph nodes.

3.2 | Intradermal injection of GFP-expression plasmid DNA with the PJI, but not a needle syringe, significantly augments the transduced GFP expression in both whole skin cells and resident DCs

To try to detect the DCs presenting the OVA peptide SIINFEKL in the MHC class I H-2K^b, FACS analysis of skin cells and draining lymph node cells using antibody specific for mouse MHC class I H-2K^b bound to OVA peptide SIINFEKL (25-D1.16)¹⁴ was performed after intradermal injection of OVA-expression plasmid DNA using the PJI or a needle syringe. However, any significantly positive cells in both skin and draining lymph node were hardly detected (Figure S3), probably due to limitation of the sensitivity. Therefore, we next used GFP-expression plasmid DNA to detect by FACS cells expressing the transduced GFP. GFP⁺ cells in whole skin cells, as well as resident DCs were detected 24 h later after injection with the PJI (Figure 2). Similarly augmented GFP expression was not observed with a needle syringe (Figure 2) nor in the draining lymph node cells 48 h later (Figure S4). Therefore, although the DCs presenting OVA peptide SIINFEKL in the MHC class I were hardly detected, these results suggested that intradermal injection of GFP-expression plasmid DNA with the PJI, but not a needle syringe, significantly augmented the transduced GFP expression in both whole skin cells and resident DCs.

3.3 | Intradermal injection of OVA-expression plasmid DNA using the PJI, but not a needle syringe, efficiently induced OVA-specific in vivo killing and antibody production

Next, we examined whether injection using the PJI would induce potent immunity, including CD8⁺ T-cell-mediated killing activity and

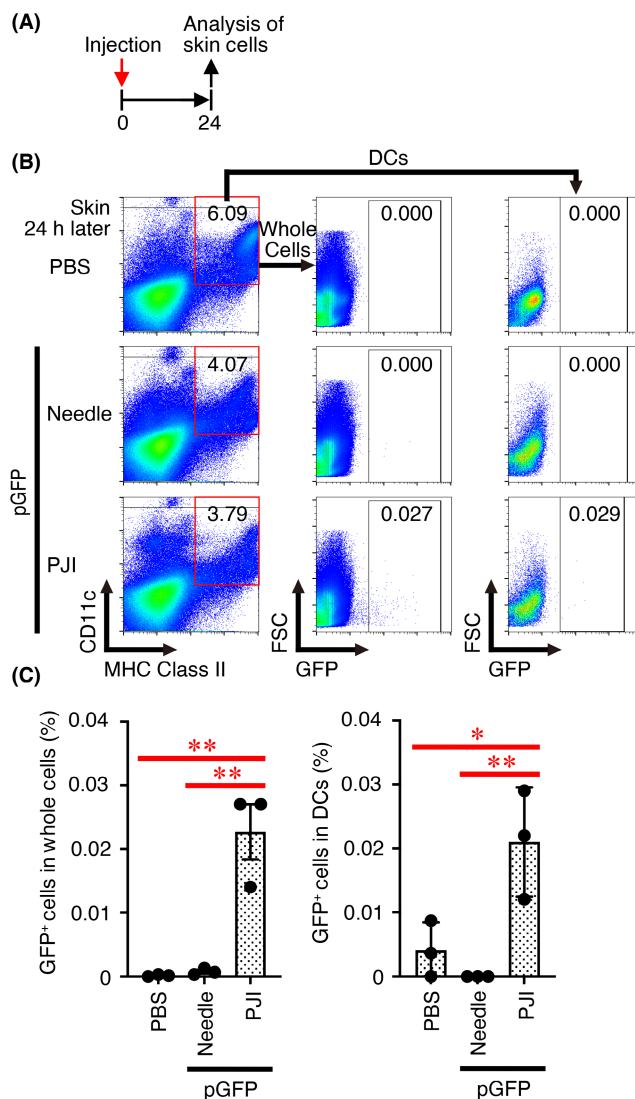


FIGURE 2 Intradermal injection of GFP-expression plasmid DNA with the pyro-drive jet injector (PJI), but not a needle syringe, significantly augmented the transduced GFP expression in both the whole skin cells and resident DCs. (A) Mice that did not receive a prior cell transfer were intradermally injected with GFP-expression plasmid DNA (pGFP) or PBS using the PJI or a needle syringe, and PBS (A). At 24 h later, the skin cells and the draining lymph node cells were analyzed for GFP expression in the whole cells or CD11c⁺ MHC class II⁺ DCs. Representative plots are shown (B), and average percentages of positive cells were calculated and compared (C). Data shown are the mean ± SEM (*n* = 3) of two independent experiments. *p*-values were determined using one-way ANOVA with the Tukey test for multiple comparisons. **p* < 0.05, ***p* < 0.01, ****p* < 0.001.

CD4⁺ T-cell-mediated antibody production. For the *in vivo* killing assay, mice that did not receive a prior cell transfer were intradermally injected using the PJI or a needle syringe twice, at a 2-week interval, with OVA-expression plasmid DNA and PBS (Figure 3A). At 1 week later, the mice received an equal number of MHC class I-restricted OVA₂₅₇₋₂₆₄ peptide-pulsed CFSE^{high} cells and unpulsed CFSE^{low} cells. OVA-specific *in vivo* killing activity in the spleen cells was then analyzed by flow cytometry. Injection using the PJI, but not a needle syringe, was associated with significant killing of the target cells *in vivo* (Figure 3B,C). For the antibody production analysis, mice that received an equal number of OT-I-derived naive CD8⁺ T cells and OT-II-derived naive CD4⁺ T cells 1 day before immunization, were intradermally injected using the PJI or a needle syringe twice, at a 2-week interval, with OVA-expression plasmid DNA, PBS, and CFA/OVA protein (Figure 4A). At 1 week later, titers of anti-OVA antibodies in serum were measured. Injection using the PJI, but not a needle syringe, was significantly associated with increased production of OVA-specific total IgG antibodies, including both the IgG2a and IgG1 subclasses (Figure 4B–D). In contrast, injection of emulsified CFA/OVA protein as a positive control enhanced the production of all OVA-specific antibodies much more. Therefore, intradermal injection of OVA-expression plasmid DNA using the PJI augments not only the CD8⁺ T-cell response, including specific CD8⁺

T-cell-mediated killing, but also the CD4⁺ T-cell response, including possible Th1 and Th2 immune responses and the resultant CD4⁺ T-cell-mediated antibody production.

3.4 | Intradermal injection of OVA-expression plasmid DNA with the PJI, but not a needle syringe, showed strong prophylactic and therapeutic effects against the progression of E.G7-OVA tumor

We next examined the protective effects of vaccination with OVA-expression plasmid DNA on the progression of the transplantable E.G7-OVA tumor. Mice that did not receive a prior cell transfer were intradermally injected using the PJI or a needle syringe twice, at a 2-week interval, with OVA-expression plasmid DNA and PBS (Figure 5A). At 1 week later, mice were subcutaneously inoculated with E.G7-OVA tumor, and tumor growth was monitored. Tumor growth was almost completely inhibited in mice injected using the PJI, but similar inhibition of tumor growth was not observed with injection using a needle syringe (Figure 5B).

We then explored the therapeutic antitumor effects of intradermal injection with OVA-expression plasmid DNA using the PJI. Mice were first inoculated with E.G7-OVA tumor. At 3 days later, the mice

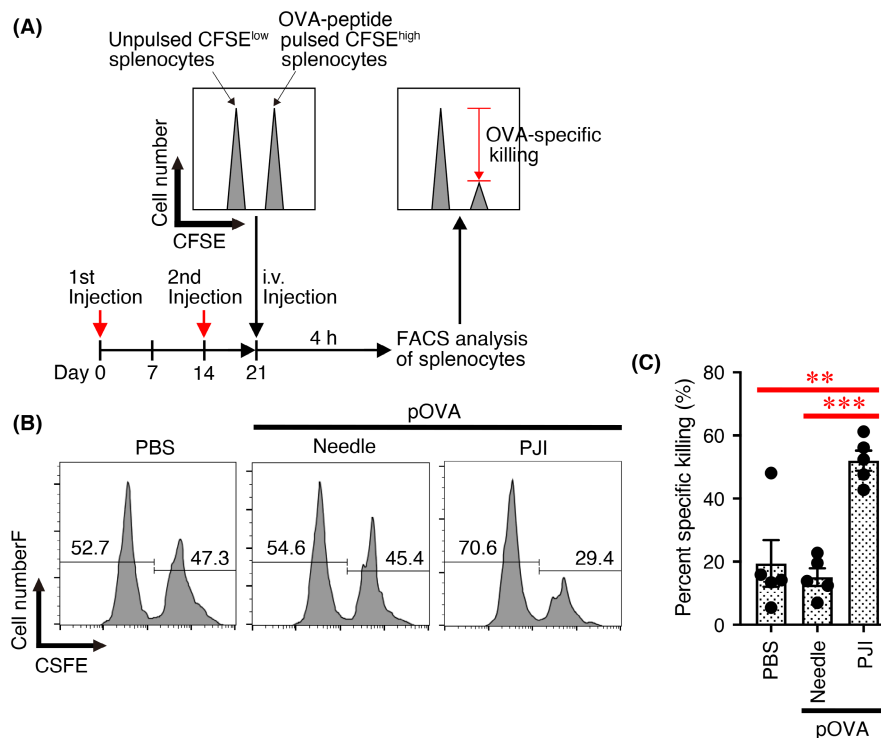


FIGURE 3 Intradermal injection of ovalbumin (OVA)-expression plasmid DNA using the pyro-drive jet injector (PJI), but not a needle syringe, efficiently induced OVA-specific *in vivo* killing in spleen cells. (A) Mice that did not receive a prior cell transfer were intradermally injected twice at a 2-week interval with OVA-expression plasmid DNA and PBS using the PJI or a needle syringe. At 1 week later, mice received an equal number of MHC class I-restricted OVA₂₅₇₋₂₆₄ peptide-pulsed CFSE^{high} cells and unpulsed CFSE^{low} cells, and OVA-specific *in vivo* killing activity in the spleen cells was analyzed by flow cytometry. (B) Representative histograms are shown, and (C) average specific killing was calculated and compared. Data shown are the mean \pm SEM ($n = 5$) of two independent experiments. p -values were determined using one-way ANOVA with the Tukey test for multiple comparisons. ** $p < 0.01$, *** $p < 0.001$.

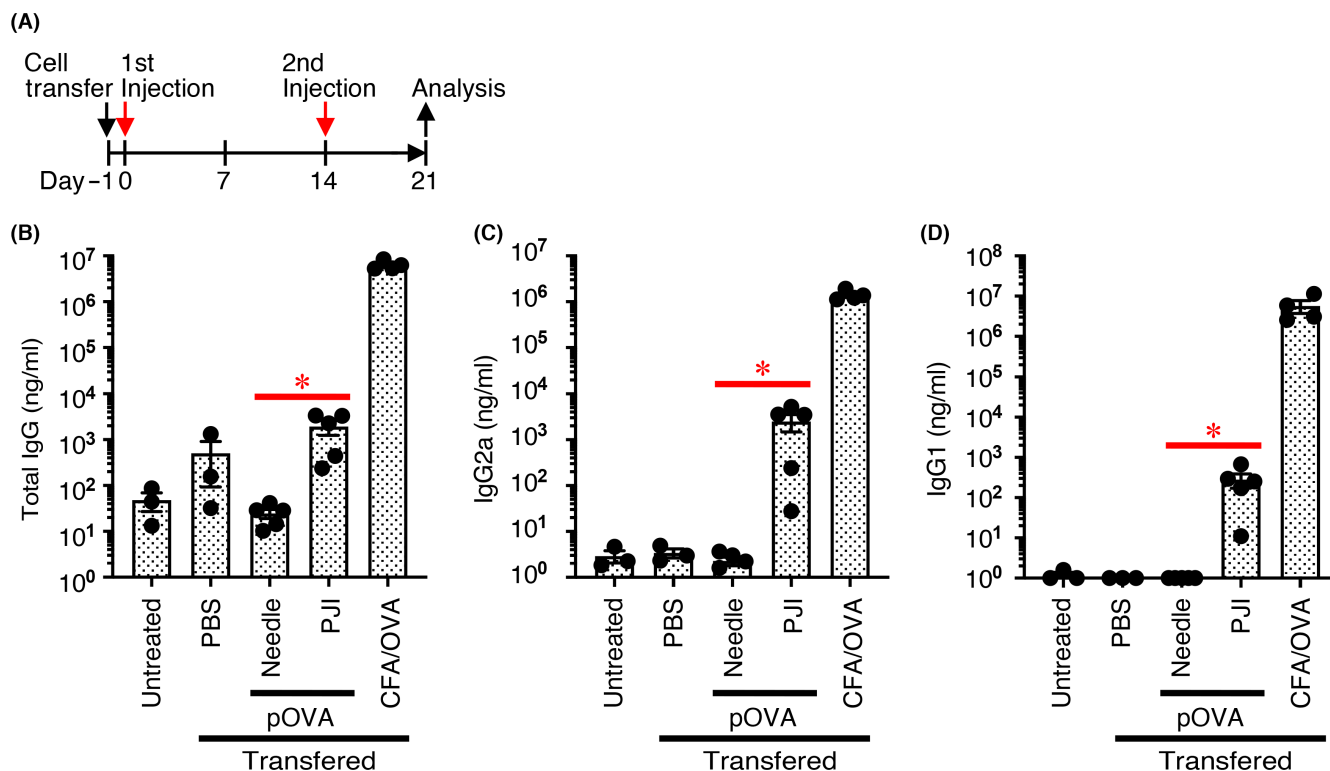


FIGURE 4 Intradermal injection of ovalbumin (OVA)-expression plasmid DNA with the pyro-drive jet injector (PJI), but not a needle syringe, efficiently increased OVA-specific antibody production of both the IgG1 and IgG2a subclasses. (A) Mice that were intravenously injected with an equal number of OT-I-derived naive CD8⁺ T cells and OT-II-derived naive CD4⁺ T cells 1 day before were then intradermally injected twice at a 2-week interval with OVA-expression plasmid DNA using the PJI or a needle syringe, PBS, and OVA protein (500 μ g) combined with complete Freund's adjuvant (CFA). At 1 week later, the titers of (B) anti-OVA total IgG antibody, and the (C) IgG2a and (D) IgG1 isotype antibodies were measured in serum. Data shown are the mean \pm SEM ($n = 5$) of three independent experiments. p -values were determined using one-way ANOVA with the Tukey test for multiple comparisons. * $p < 0.05$.

were intradermally injected with OVA-expression plasmid DNA and PBS using the PJI or a needle syringe, and tumor growth was monitored (Figure 5C). Again, tumor growth was significantly inhibited in mice injected using the PJI, but not in those injected using a needle syringe (Figure 5D). Therefore, intradermal injection using the PJI, but not a needle syringe, showed a strong prophylactic effect as well as a therapeutic effect against the progression of transplantable tumor.

3.5 | The prophylactic effect against the progression of E.G7-OVA tumor was stronger after intradermal injection of OVA-expression plasmid DNA using the PJI than after injection of CFA/OVA protein or alum/OVA protein

CFA is a water-in-oil emulsion containing an antigen and inactivated *Mycobacterium tuberculosis*. It is widely used in rodents and is considered to be the most effective adjuvant available for consistent production of high-titer antibodies.^{18–20} AlumVax is a wet colloidal gel of 2% aluminum hydroxide that is the adjuvant most commonly used in approved prophylactic vaccines for humans because of its excellent safety profile and ability to enhance the protective humoral immune

response.^{20–22} We therefore assessed the prophylactic antitumor effects of intradermal injection with OVA-expression plasmid DNA and with those frequently used adjuvants. Mice that did not receive a prior cell transfer were intradermally injected with OVA-expression plasmid DNA using the PJI or a needle syringe, alum/OVA protein, or CFA/OVA protein. At 1 week later, mice were subcutaneously inoculated with E.G7-OVA tumor, and tumor growth was monitored (Figure 6A). Tumor progression was significantly inhibited only after intradermal injection of OVA-expression plasmid DNA using the PJI and not after intradermal injection of CFA/OVA protein or alum/OVA protein (Figure 6B). To examine the molecular mechanism, depletion experiments using anti-CD4, anti-CD8, or control IgG were performed (Figure 6C). The depletion of CD8⁺ T cells, but not CD4⁺ T cells, completely reversed the prophylactic effect (Figure 6D). These results suggest that the prophylactic effect against the progression of E.G7-OVA tumor is stronger with intradermal injection of OVA-expression plasmid DNA than with injection of CFA/OVA protein or alum/OVA protein, and that induction of CTLs is important for the prophylactic effect, and that the antibody response may not be necessary for this effect under experimental conditions.

To further investigate any difference in the induction of antitumor responses between OVA-expression plasmid DNA with the PJI, CFA/OVA protein, and alum/OVA protein, we next focused on CD8⁺

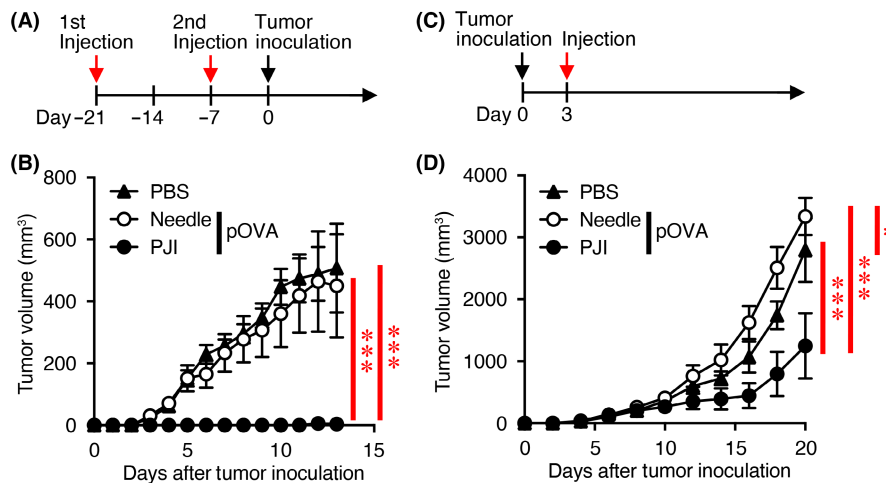


FIGURE 5 Intradermal injection of ovalbumin (OVA)-expression plasmid DNA with the pyro-drive jet injector (PJI), but not a needle syringe, showed strong prophylactic and therapeutic effects against the progression of the E.G7-OVA tumor. (A) Mice that did not receive a prior cell transfer were intradermally injected twice at a 2-week interval with OVA-expression plasmid DNA using the PJI or a needle syringe, and PBS. (B) At 1 week later, mice were subcutaneously inoculated with E.G7-OVA tumor, and tumor growth was monitored. (C) At 3 days after inoculation with E.G7-OVA tumor, mice were injected intradermally with OVA-expression plasmid DNA and PBS using the PJI or a needle syringe, and (D) tumor growth was monitored. Data shown are the mean \pm SEM ($n = 5$) of two independent experiments. p -values were determined using two-way ANOVA with Tukey test for multiple comparisons. * $p < 0.05$, *** $p < 0.001$.

T cells and performed time kinetic analysis on the frequency of OVA-specific CD8⁺ T cells induced in nontransferred mice after a single injection of these cells (Figure 6E). The frequency of OVA-specific CD8⁺ T cells was rapidly increased 7 days after the injection of alum/OVA protein but gradually decreased thereafter (Figure 6F,G). However, the injection of CFA/OVA protein did not significantly increase the frequency (Figure 6F,G). In contrast, the frequency of OVA-specific CD8⁺ T cells started to increase more than 7 days later after injection with PJI, was greatly enhanced on day 14, and gradually decreased thereafter (Figure 6F,G). Therefore, these results suggest that the induction of OVA-specific CD8⁺ T cells by PJI is likely to take more time than that by alum/OVA protein, but be higher. In contrast, OVA-specific CD8⁺ T cells were hardly induced by injection with CFA/OVA protein in nontransferred mice. CFA should be effective for the induction of antitumor effects via antibodies.^{18–20}

3.6 | Multiple intradermal injections of OVA-expression plasmid DNA with the PJI efficiently generated OVA-specific CD8⁺ T cells compared with those with alum/OVA

Finally, to further explore the mechanism whereby PJI induces the potent antitumor effects, the time kinetic analysis on the generation of OVA-specific CD8⁺ T cells after multiple injections was compared among OVA-expression plasmid DNA with PJI, CFA/OVA, and alum/OVA protein. Mice that did not receive a prior cell transfer were intradermally injected one to three times at a 2-week interval with OVA-expression plasmid DNA using the PJI or a needle syringe together with PBS, OVA protein (both 50 μ g) combined with CFA/OVA or alum/OVA (Figure 7A). At 1 week later after each injection,

the draining lymph node cells were stained with OVA-specific MHC class I tetramer and anti-CD8. Even 1 week after the first injection with the PJI, the frequency of OVA-specific CD8⁺ T cells tended to increase, after two injections the frequency greatly enhanced, and after three injections the frequency was still kept high (Figure 7B,C). In contrast, for alum/OVA the frequency rapidly increased after the first injection and gradually decreased thereafter (Figure 7B,C). Again, the injection of CFA/OVA protein did not significantly increase the frequency (Figure 7B,C). Therefore, consistent with the results in Figure 6E,F, the time kinetics to induce the generation of OVA-specific CD8⁺ T cells differed among them, and the effect of PJI was slightly slower, but the maximum induction level by PJI is higher than that by alum/OVA, which could explain the different outcomes between them for the antitumor effects.

4 | DISCUSSION

In the present study, we used OVA as a model antigen and OVA-expressing transplantable tumor E.G7-OVA to investigate the potential use of a novel needle-free PJI for vaccination against cancers. First, flow cytometry analysis using tetramers of MHC class I H-2K^b and its OVA peptide and MHC class II I-A^b and its OVA peptide revealed that, 1 week later, OVA-specific CD8⁺ T-cell expansion was greatly augmented after intradermal injection of OVA-expression plasmid DNA into transferred mice using the PJI, but not after injection using a needle syringe (Figure 1B,C). In contrast, expansion of OVA-specific CD4⁺ T cells was barely detectable with a tetramer of MHC class II I-A^b and its OVA peptide (Figure 1C,E). This could be because the plasmid DNA rapidly activates the MHC class I pathway and subsequent cellular immune

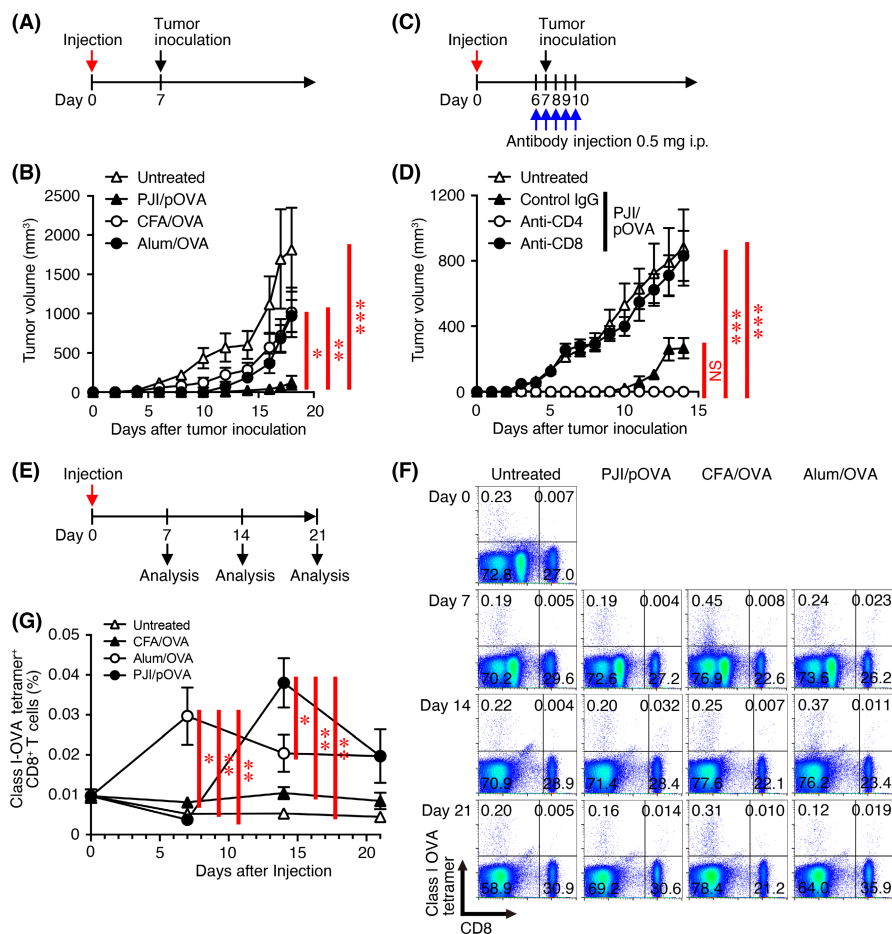


FIGURE 6 The prophylactic effect against the progression of E.G7-OVA tumor was stronger after intradermal injection of ovalbumin (OVA)-expression plasmid DNA using the pyro-drive jet injector (PJI) compared with after injection of OVA protein combined with complete Freund's adjuvant (CFA/OVA, 500 μ g) or OVA protein combined with alum (alum/OVA, 50 μ g). (A) Mice that did not receive prior cell transfer were intradermally injected once with OVA-expression plasmid DNA using the PJI, CFA/OVA and alum/OVA protein. (B) At 1 week later, mice were subcutaneously inoculated with E.G7-OVA tumor, and tumor growth was monitored. Data shown are the mean \pm SEM ($n = 5$) of two independent experiments. (C, D) For depletion of CD4⁺ T cells or CD8⁺ T cells, each mouse was injected i.p. with 0.5 mg rat antimouse CD8, anti-CD4, or normal rat IgG as control antibody in 200 μ l PBS 1 day before tumor inoculation, once daily for the following 5 consecutive days, and tumor growth was monitored. Data shown are the mean \pm SEM ($n = 5$). (E–G) For time kinetic analysis on the induction of OVA-specific CD8⁺ T cells, mice that did not receive prior cell transfer were intradermally injected once with OVA-expression plasmid DNA using the PJI and with CFA/OVA, and Alum/OVA. On days 0, 7, 14, and 21, the draining lymph node cells were stained with OVA-specific MHC class I tetramer and anti-CD8. Representative plots are shown (F), and average percentages of positive cells were calculated and compared (G). Data shown are the mean \pm SEM ($n = 3$ –5) of two independent experiments. p -values were determined using two-way ANOVA with the Tukey test for multiple comparisons. * $p < 0.05$, ** $p < 0.01$, *** $p < 0.001$.

responses, whereas it may take more time to activate the MHC class II pathway and subsequent humoral immune responses.²³ This is because plasmid DNA has to be transcribed and translated to protein, which is then phagocytosed by DCs and subsequently activates the MHC class II pathway.²³ Use of the PJI was associated not only with augmented IFN- γ mRNA expression, but also augmented IL-4 mRNA expression in draining lymph node cells in transferred mice (Figure 1F,G). But, in nontransferred mice, intracellular cytokine staining analyses revealed that PJI augmented the frequency of only IFN- γ ⁺CD8⁺ T cells but not IFN- γ ⁺CD4⁺ T cells, suggesting the differentiation into Tc1 cells (Figure S5). Consistent with these results, with respect to OVA-specific recall responses, proliferation of draining lymph node cells was greatly induced by

MHC class I-restricted OVA_{257–264} peptide and slightly induced by MHC class II-restricted OVA_{323–339} peptide (Figure 1H,I). These results suggested that an OVA-specific CD8⁺ T-cell response is much more quickly and efficiently induced and an OVA-specific CD4⁺ T-cell response is reasonably induced in the draining lymph nodes with intradermal injection of OVA-expression plasmid DNA using the PJI. Moreover, OVA-specific in vivo killing of the target cells was significantly increased (Figure 3B,C), and greatly enhanced OVA-specific antibody production of both the IgG2a and IgG1 subclasses was also observed (Figure 4C,D). These results suggested that the intradermal injection of OVA-expression plasmid DNA using the PJI augments not only the CD8⁺ T-cell response, but also the CD4⁺ T-cell response, including both the Th1 and Th2 immune

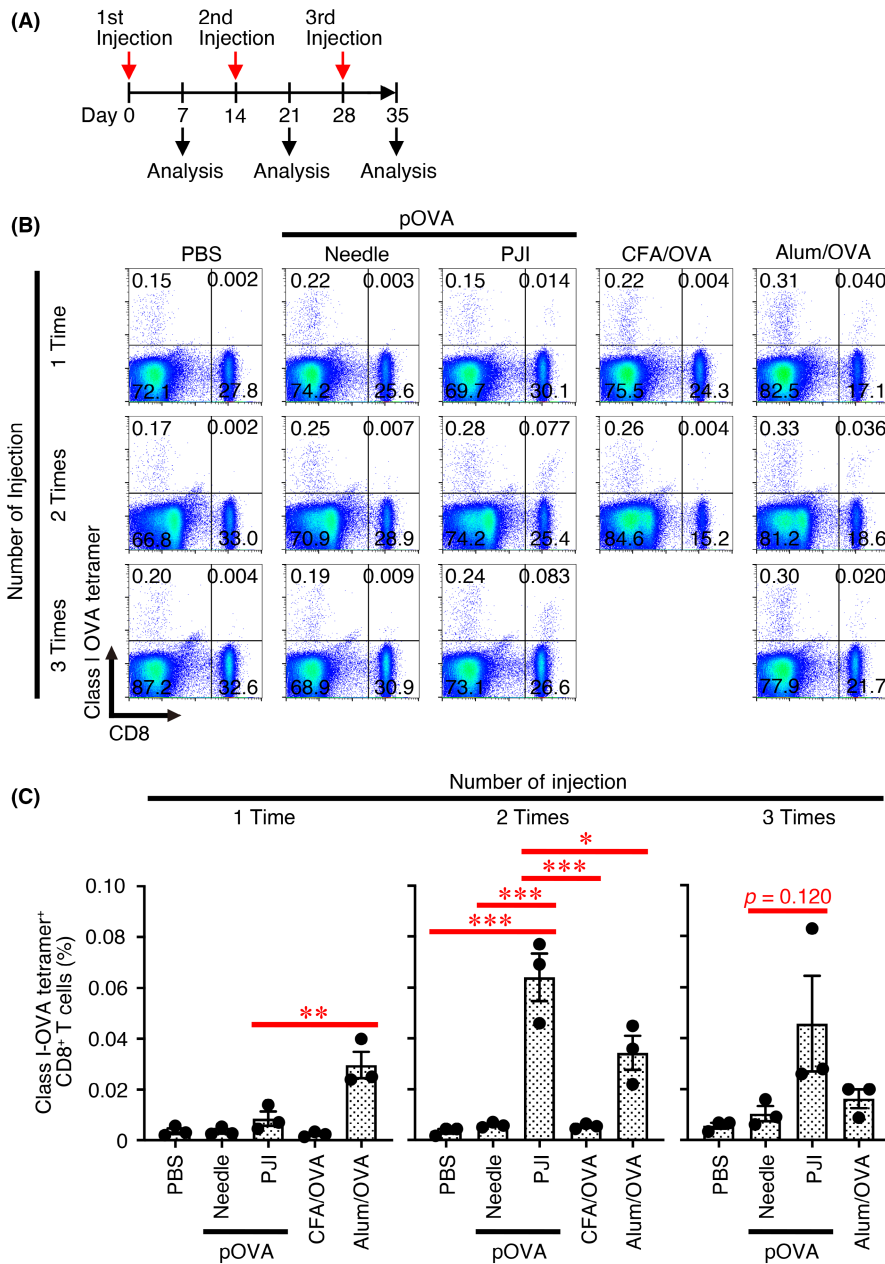


FIGURE 7 Multiple intradermal injections of ovalbumin (OVA)-expression plasmid DNA with the pyro-drive jet injector (PJI) efficiently generated OVA-specific CD8⁺ T cells compared with those with OVA protein combined with alum (alum/OVA). (A) Mice that did not receive a prior cell transfer were intradermally injected one to three times at a 2-week interval with OVA-expression plasmid DNA and PBS using the PJI or a needle syringe together with OVA protein combined with complete Freund's adjuvant (CFA/OVA, 50 μ g) or alum/OVA (50 μ g). At 1 week later after each injection, the draining lymph node cells were stained with OVA-specific MHC class I tetramer and anti-CD8. Representative plots are shown (B), and average percentages of positive cells were calculated and compared (C). Data shown are the mean \pm SEM ($n = 3$) of two independent experiments. p -values were determined using one-way ANOVA with Tukey test for multiple comparisons. * $p < 0.05$, ** $p < 0.01$, *** $p < 0.001$.

responses. Notably, intradermal injection of OVA-expression plasmid DNA using the PJI, but not a needle syringe, twice at a 2-week interval showed a strong prophylactic antitumor effect on the progression of transplantable E.G7-OVA tumor (Figure 5A,B). The strong prophylactic antitumor effect was likely to be attributable to the induction of OVA-specific CTLs and production of antibodies. Intriguingly, a strong therapeutic effect was also observed when mice were first inoculated with the E.G7-OVA tumor and, just 3 days later, intradermally injected with OVA-expression plasmid DNA using the PJI (Figure 5C,D). Moreover, even when compared with the well known and frequently used adjuvants CFA¹⁸⁻²⁰ and alum,²⁰⁻²² combined with OVA protein, the prophylactic effect against the tumor was stronger with intradermal injection using the PJI 1 week later (Figure 6B) in a CD8⁺ T-cell-dependent, but not a CD4⁺ T-cell-dependent, manner (Figure 6C,D). Given the very short

time between injection using the PJI and tumor inoculation, the observed therapeutic effects are therefore mainly a result of prompt and strong generation of OVA-specific CTLs associated with use of the PJI. Moreover, the time kinetics to induce the generation of OVA-specific CD8⁺ T cells after a single injection (Figure 6E-G) and multiple injections (Figure 7) is different among OVA-expression plasmid DNA with PJI, CFA/OVA protein, and alum/OVA protein. The induction of OVA-specific CD8⁺ T cells by PJI is slightly slower compared with alum/OVA protein, probably because it may take time to transcribe and translate DNA to produce protein (Figure S6) in DCs and activate MHC class I pathway, compared with injected protein, which is then phagocytosed by DCs and activates the cross-presentation pathway. But, the maximum induction level by PJI is higher than that by CFA/OVA or alum/OVA, which could explain the higher prophylactic antitumor effects (Figures 6 and

7). In the experiment in Figure 6, we used OVA protein 500 μg for CFA, which may be the maximum condition, and 50 μg for alum, which is recommended to use for alum according to the manufacturer's instruction, and in the experiment in Figure 7, we used equal amounts of OVA protein, 50 μg , for both CFA and alum for comparison. In both cases, CFA/OVA hardly induced strong CD8⁺ T-cell-mediated immune responses, although it induced strong antibody production (Figure 4).¹⁸⁻²⁰ In addition, it was not easy to adjust the same experimental conditions between OVA-expression plasmid DNA with PJI and CFA/OA or alum/OVA protein, because the former was plasmid DNA that preferentially activates the MHC class I pathway²³ and the latter is protein with adjuvants that preferentially activates the MHC class II pathway.¹⁸⁻²² Therefore, we used them under respective optimal conditions as much as possible. Therefore, our results suggested that novel needle-free PJI is a promising tool for DNA vaccination, inducing a prophylactic effect and demonstrating a therapeutic effect against cancer, likely to be because of prompt and strong generation of antigen-specific CTLs and the subsequent production of antibodies of both of the IgG2a and IgG1 isotypes.

Previously, we compared the efficiency of the PJI and a needle syringe to deliver plasmid DNAs of luciferase or OVA into the skin and to induce subsequent protein expression.¹⁰ Protein expression in the skin was ~10 times higher with use of the PJI than with a needle syringe, likely to be because plasmid DNA injected intradermally using the PJI spreads widely through the dermis from the epidermis, while plasmid DNA injected using a needle syringe spreads only within the central area of the dermis.¹⁰ Also, compared with use of a needle syringe, use of the PJI effectively introduces the plasmid DNA into the nucleus at a higher frequency.¹⁰ Although this explanation accounts for the efficient induction of OVA-specific CTLs with the use of the PJI, whether resident DCs in the epidermis such as Langerhans cells and dermal DCs are indeed preferentially induced after injection of plasmid DNA using the PJI rather than a needle syringe remains to be clarified. Because the injection power of the PJI is primed by gunpowder, the injection occurs at very high flow rate (approximately 1 ml s⁻¹),¹² and the flow rate for injection with a needle syringe is less than 0.025 ml s⁻¹.²⁴ Because the injection flow rate affects subsequent protein expression,²⁴ the much higher injection flow rate with the PJI than with a needle syringe is likely to account for the augmented protein expression. Notably, the transfection efficiency of plasmid DNA with cationic liposomes was previously demonstrated to be dramatically enhanced by shear stress²⁵—that is, stress applied parallel or tangential to the surface of cells—and to regulate cell physiology, facilitating endocytosis, and uptake of extracellular molecules.^{26,27} A possible explanation is the induction of torsion in the hydrophilic lipid in the cellular membrane, resulting in instability of the membrane bilayer and the formation of transient pores in the membrane.²⁸⁻³⁰ Intriguingly, that hypothesis has led to the approach of taking advantage of shear-induced cell deformation to deliver biomolecules such as plasmid DNAs, RNAs, and proteins into the cellular cytosol or nucleus through the microfluidic or nanofluidic system.³⁰ Consistent with those reports, shear stress caused

by the rapid flow rate with the PJI was recently demonstrated to increase the endocytosis of plasmid DNA and its internalization into cells, resulting in enhanced protein expression.³¹

After the plasmid DNA is intradermally injected into the skin using the PJI, DNA uptake occurs via the endocytosis pathway in cells such as Langerhans cells and dermal DCs, keratinocytes, and other somatic cells located in the epidermis and dermis. In skin-resident DCs, protein is endogenously expressed by the plasmid DNA, processed into small peptides, and efficiently presented on MHC class I molecules that strongly activate antigen-specific CD8⁺ T cells and generate their CTLs. In contrast, in other somatic cells, the protein is endogenously expressed by the plasmid DNA, and its secreted protein or dead cells expressing the protein are phagocytosed by the skin-resident DCs. The DCs then process the protein into small peptides and efficiently present them on MHC class II molecules, which activate antigen-specific CD4⁺ T cells, and also on MHC class I molecules via the cross-presentation pathway,³² which activates antigen-specific CD8⁺ T cells. Therefore, the properties of the PJI as discussed earlier contrast considerably with the properties of an antigen protein combined with Alum or CFA. Injection of plasmid DNA using the PJI directly activates mainly the MHC class I pathway and subsequent cellular immunity, while an antigen protein with Alum or CFA activates mainly the MHC class II pathway and subsequent humoral immunity, together with the MHC class I pathway via the cross-presentation pathway. Moreover, alum markedly induces the generation of Th2 cytokines including IL-4, resulting in the production of the IgG1 isotype antibody,³³ and CFA preferably activates Th1 cells secreting IFN- γ .³⁴

Gene delivery systems are mainly categorized into two groups: viral or nonviral vector-based delivery and physical delivery.^{35,36} The latter includes electroporation,³⁷ ultrasound method,³⁸ needle-free injector,³⁹ gene gun,⁴⁰ microneedle,^{36,41} microfluidic or nanofluidic system,³⁰ and so on. Biodegradable microneedle is a pain-free method for delivering DNA across the skin in a slow-releasing manner.^{36,41} Although various types of devices for needle-free injectors have been developed, only the pyro-drive one is ours.³⁹ Because other needle-free injectors utilize spring or compressed gas as an actuation mechanism,³⁹ the flow rate for injection of the PJI would be higher than others. The gene gun is a device used for gene delivery by bombarding the target cells with DNA-coated microparticles such as high-density gold.³⁰ The DNA-coated gold microparticles are accelerated to high velocity by helium gas pressure and penetrated through cell membranes into the target cells. The gene gun was originally developed to deliver gene through cell walls into plant cells.⁴⁰ It was previously reported that gene delivery by gene gun is superior in the ability to induce CTLs and humoral immune responses to that of jet injector or needle syringe.^{42,43} However, for clinical application to humans, PJI should be better because it is compact and safe in that there is no risk of microparticles remaining in the body after injection, as with the gene gun, although further studies are necessary to prove the efficacy and safety in humans.

Considering the evidence overall, the present study suggests that intradermal vaccination with OVA-expression plasmid DNA using the

PJI, but not a needle syringe, induces a strong antitumor immune response via enhanced generation of antigen-specific CTLs, with subsequent killing of the target cells, and that efficient antigen-specific antibody production is also enhanced. Notably, induction of prophylactic antitumor immunity was faster and stronger with the injection of OVA-expression plasmid DNA using the PJI than with the injection of OVA protein combined with alum or CFA. This observation is probably attributable to higher uptake of DNA and the consequent efficiently increased protein expression by resident DCs in the skin and efficient migration and augmentation of DC maturation in the draining lymph nodes to generate antigen-specific CTLs. The novel needle-free PJI is therefore a promising tool for DNA, and possibly mRNA, vaccination to induce potent antitumor immunity against cancers.

AUTHOR CONTRIBUTIONS

Shinya Inoue, Izuru Mizoguchi, Kunihiko Yamashita, and Takayuki Yoshimoto designed the study; Shinya Inoue, Izuru Mizoguchi, Jukito Sonoda, Eri Sakamoto, Yasuhiro Katahira, Hideaki Hasegawa, Aruma Watanabe, and Yuma Furusaka performed the experiments; Shinya Inoue, Izuru Mizoguchi, Jukito Sonoda, and Eri Sakamoto analyzed the data; Naoki Sakaguchi, Kazuhiro Terai, and Kunihiko Yamashita contributed the reagents used in the study; Mingli Xu, Toshihiko Yoneto, Naoki Sakaguchi, Kazuhiro Terai, Kunihiko Yamashita, and Takayuki Yoshimoto discussed the data; Shinya Inoue, Izuru Mizoguchi, and Takayuki Yoshimoto wrote the manuscript. All authors have read and approved the final manuscript.

ACKNOWLEDGMENTS

The authors thank Dr. K. Takahashi (Yokohama City University), Dr. T. Yoshimoto (Hyogo Medical University), Dr. J. Miyazaki (Osaka University), and the Animal Research Center of Tokyo Medical University for OT-I TCR transgenic mice, OT-II TCR transgenic mice, pCAGGS, and animal care.

FUNDING INFORMATION

This study was supported by grants from the Grant-in-Aid for Scientific Research from the Ministry of Education, Culture, Sports, Science, and Technology, Japan, and from Daicel Corporation.

CONFLICT OF INTEREST

T. Yoshimoto received a research grant from Daicel Corporation. N. S., K. T., and K. Y. are employees of Daicel Corporation. The other authors have no conflict of interest. None of us are Editorial Board Member of Cancer Science.

ETHICS STATEMENT

Approval of the research protocol by an Institutional Reviewer Board: N/A. Informed Consent: N/A. Registry and the Registration No. of the study/trial: N/A. Animal Studies: Animal Studies, all animal experiments were approved by the President and the Institutional Animal Care and Use Committee of Tokyo Medical University and were performed in accordance with institutional, scientific

community, and national guidelines for animal experimentation and the Animal Research: Reporting of In Vivo Experiments guidelines.

ORCID

Takayuki Yoshimoto  <https://orcid.org/0000-0002-2847-0341>

REFERENCES

- Jiang Y, Wu Q, Song P, You C. The variation of SARS-CoV-2 and advanced research on current vaccines. *Front Med (Lausanne)*. 2021;8:806641.
- Shafaati M, Saidijam M, Soleimani M, et al. A brief review on DNA vaccines in the era of COVID-19. *Future Virol*. 2021;17:49-66.
- Migliore A, Gigliucci G, Di Marzo R, Russo D, Mammucari M. Intradermal vaccination: a potential tool in the Battle against the COVID-19 pandemic? *Risk Manag Healthc Foreign Policy*. 2021;14:2079-2087.
- Roukens AH, Gelinck LB, Visser LG. Intradermal vaccination to protect against yellow fever and influenza. *Curr Top Microbiol Immunol*. 2012;351:159-179.
- Zehrung D, Jarrahan C, Wales A. Intradermal delivery for vaccine dose sparing: overview of current issues. *Vaccine*. 2013;31(34):3392-3395.
- Egunsola O, Clement F, Taplin J, et al. Immunogenicity and safety of reduced-dose intradermal vs intramuscular influenza vaccines: a systematic review and meta-analysis. *JAMA Netw Open*. 2021;4(2):e2035693.
- Liang F, Lindgren G, Lin A, et al. Efficient targeting and activation of antigen-presenting cells in vivo after modified mRNA vaccine Administration in Rhesus Macaques. *Mol Ther*. 2017;25(12):2635-2647.
- Yu C, Walter M. Needleless injectors for the administration of vaccines: a review of clinical effectiveness. 2020.
- Miyazaki H, Atobe S, Suzuki T, Iga H, Terai K. Development of pyro-drive jet injector with controllable jet pressure. *J Pharm Sci*. 2019;108(7):2415-2420.
- Chang C, Sun J, Hayashi H, et al. Stable immune response induced by intradermal DNA vaccination by a novel needleless pyro-drive jet injector. *AAPS PharmSciTech*. 2019;21(1):19.
- Nakae T, Obana M, Maeda T, et al. Gene transfer by pyro-drive jet injector is a novel therapeutic approach for muscle diseases. *Gene*. 2021;788:145664.
- Miyazaki H, Sakaguchi Y, Terai K. Potent intradermal gene expression of naked plasmid DNA in pig skin following pyro-drive jet injection. *J Pharm Sci*. 2021;110(3):1310-1315.
- Niwa H, Yamamura K, Miyazaki J. Efficient selection for high-expression transfectants with a novel eukaryotic vector. *Gene*. 1991;108(2):193-199.
- Porgador A, Yewdell JW, Deng Y, Bennink JR, Germain RN. Localization, quantitation, and in situ detection of specific peptide-MHC class I complexes using a monoclonal antibody. *Immunity*. 1997;6(6):715-726.
- Schneider CA, Rasband WS, Eliceiri KW. NIH image to ImageJ: 25 years of image analysis. *Nat Methods*. 2012;9(7):671-675.
- Kim MV, Ouyang W, Liao W, Zhang MQ, Li MO. Murine in vivo CD8+ T cell killing assay. *Bio-Protocol*. 2014;4(13):e1172.
- Hisada M, Kamiya S, Fujita K, et al. Potent antitumor activity of interleukin-27. *Cancer Res*. 2004;64(3):1152-1156.
- Billiau A, Matthys P. Modes of action of Freund's adjuvants in experimental models of autoimmune diseases. *J Leukoc Biol*. 2001;70(6):849-860.
- Awate S, Babiuk LA, Mutwiri G. Mechanisms of action of adjuvants. *Front Immunol*. 2013;4:114.

20. Sarkar I, Garg R, van Drunen Littel-van den Hurk S. Selection of adjuvants for vaccines targeting specific pathogens. *Expert Rev Vaccines*. 2019;18(5):505-521.
21. Brunner R, Jensen-Jarolim E, Pali-Scholl I. The ABC of clinical and experimental adjuvants—a brief overview. *Immunol Lett*. 2010;128(1):29-35.
22. Danielsson R, Eriksson H. Aluminium adjuvants in vaccines—a way to modulate the immune response. *Semin Cell Dev Biol*. 2021;115:3-9.
23. Shedlock DJ, Weiner DB. DNA vaccination: antigen presentation and the induction of immunity. *J Leukoc Biol*. 2000;68(6):793-806.
24. Andre FM, Cournil-Henrionnet C, Vernerey D, Opolon P, Mir LM. Variability of naked DNA expression after direct local injection: the influence of the injection speed. *Gene Ther*. 2006;13(23):1619-1627.
25. Fujiwara T, Akita H, Furukawa K, Ushida T, Mizuguchi H, Harashima H. Impact of convective flow on the cellular uptake and transfection activity of lipoplex and adenovirus. *Biol Pharm Bull*. 2006;29(7):1511-1515.
26. Hallow DM, Seeger RA, Kamaev PP, Prado GR, LaPlaca MC, Prausnitz MR. Shear-induced intracellular loading of cells with molecules by controlled microfluidics. *Biotechnol Bioeng*. 2008;99(4):846-854.
27. Sharei A, Zoldan J, Adamo A, et al. A vector-free microfluidic platform for intracellular delivery. *Proc Natl Acad Sci USA*. 2013;110(6):2082-2087.
28. Mardikar SH, Niranjana K. Observations on the shear damage to different animal cells in a concentric cylinder viscometer. *Biotechnol Bioeng*. 2000;68(6):697-704.
29. Hanasaki I, Walther JH, Kawano S, Koumoutsakos P. Coarse-grained molecular dynamics simulations of shear-induced instabilities of lipid bilayer membranes in water. *Phys Rev E Stat Nonlin Soft Matter Phys*. 2010;82(5 Pt 1):051602.
30. Hur J, Chung AJ. Microfluidic and nanofluidic intracellular delivery. *Adv Sci (Weinh)*. 2021;8(15):e2004595.
31. Miyazaki H, Ogura M, Sakaguchi Y, Hasegawa T, Atobe S, Terai K. Mechanism of jet injector-induced plasmid DNA uptake: contribution of shear stress and endocytosis. *Int J Pharm*. 2021;609:121200.
32. Embgenbroich M, Burgdorf S. Current concepts of antigen cross-presentation. *Front Immunol*. 2018;9:1643.
33. Mancino D, Ovary Z. Adjuvant effects of amorphous silica and of aluminium hydroxide on IgE and IgG1 antibody production in different inbred mouse strains. *Int Arch Allergy Appl Immunol*. 1980;61(3):253-258.
34. Zheng CL, Ohki K, Hossain A, Kukita A, Satoh T, Kohashi O. Complete Freund's adjuvant promotes the increases of IFN-gamma and nitric oxide in suppressing chronic arthritis induced by pristane. *Inflammation*. 2003;27(4):247-255.
35. Al-Dosari MS, Gao X. Nonviral gene delivery: principle, limitations, and recent progress. *AAPS J*. 2009;11(4):671-681.
36. Chen W, Li H, Shi D, Liu Z, Yuan W. Microneedles as a delivery system for gene therapy. *Front Pharmacol*. 2016;7:137.
37. Sardesai NY, Weiner DB. Electroporation delivery of DNA vaccines: prospects for success. *Curr Opin Immunol*. 2011;23(3):421-429.
38. Ng CK, Putra SL, Kennerley J, et al. Genetic engineering biofilms in situ using ultrasound-mediated DNA delivery. *J Microbial Biotechnol*. 2021;14(4):1580-1593.
39. Han HS, Hong JY, Kwon TR, et al. Mechanism and clinical applications of needle-free injectors in dermatology: literature review. *J Cosmet Dermatol*. 2021;20(12):3793-3801.
40. Bergmann-Leitner ES, Leitner WW. Vaccination using Gene-gun Technology. *Methods Mol Biol*. 2015;1325:289-302.
41. Menon I, Bagwe P, Gomes KB, et al. Microneedles: a new generation vaccine delivery system. *Micromachines (Basel)*. 2021;12(4):435.
42. Nguyen-Hoai T, Kobelt D, Hohn O, et al. HER2/neu DNA vaccination by intradermal gene delivery in a mouse tumor model: gene gun is superior to jet injector in inducing CTL responses and protective immunity. *Oncotargets Ther*. 2012;1(9):1537-1545.
43. Trimble C, Lin CT, Hung CF, et al. Comparison of the CD8+ T cell responses and antitumor effects generated by DNA vaccine administered through gene gun, biojector, and syringe. *Vaccine*. 2003;21(25-26):4036-4042.

SUPPORTING INFORMATION

Additional supporting information can be found online in the Supporting Information section at the end of this article.

How to cite this article: Inoue S, Mizoguchi I, Sonoda J, et al. Induction of potent antitumor immunity by intradermal DNA injection using a novel needle-free pyro-drive jet injector. *Cancer Sci*. 2023;114:34-47. doi: [10.1111/cas.15542](https://doi.org/10.1111/cas.15542)